

## The Effect of Zeolite Features on Catalytic Performances of CuZnZr/Zeolite Hybrid Catalysts in One-pot CO<sub>2</sub>-to-DME Hydrogenation

Enrico Catizzone<sup>1\*</sup>, Giuseppe Bonura<sup>2</sup>, Massimo Migliori<sup>3</sup>, Giacobbe Braccio<sup>1</sup>, Francesco Frusteri<sup>2</sup>, Girolamo Giordano<sup>3</sup>

<sup>1</sup> ENEA-Italian National Agency for New Technologies, Energy and Sustainable Economic Development, Trisaia Research Centre, I-75026, Rotondella, Italy

<sup>2</sup> CNR-ITAE, Istituto di Tecnologie Avanzate per l'Energia "Nicola Giordano", via S. Lucia Sopra Contesse, 5, I-98126, Messina, Italy

<sup>3</sup> University of Calabria, Dept. of Environmental and Chemical Engineering, via P. Bucci, 44a, I-87036, Rende, Italy

Corresponding Author Email: [enrico.catizzone@enea.it](mailto:enrico.catizzone@enea.it)

<https://doi.org/10.18280/ti-ijes.632-420>

### ABSTRACT

**Received:** 28 January 2019

**Accepted:** 24 April 2019

#### Keywords:

CO<sub>2</sub> recycling, dimethyl ether, heterogeneous catalysis, zeolites

The production of DME from CO<sub>2</sub> hydrogenation is a way of recycling CO<sub>2</sub> and it requires the use of a hybrid multifunctional catalyst to efficiently catalyze the two consecutive reaction paths of methanol synthesis and methanol dehydration directly in one single step. The aim of this work is to investigate the utilization of zeolite-based catalysts for dimethyl ether synthesis by assessing the role of catalyst features in both methanol dehydration and one-pot CO<sub>2</sub> hydrogenation.

Obtained results, discussed in terms of turnover frequency reveal that FER-type zeolite prepared with Si/Al=10 exhibits the best performances during vapor-phase methanol dehydration whilst the efficiency of CO<sub>2</sub>-to-DME process strongly depends on the way in which metallic and acidic materials are coupled. Single grain prepared via gel-oxalate precipitation of CuZnZr over zeolite crystals exhibit the best performances in terms of CO<sub>2</sub> conversion and DME productivity.

## 1. INTRODUCTION

The utilization of CO<sub>2</sub> as carbon source represents a reliable strategy to recycle "environmentally unfriendly" compounds in the production chain of chemicals currently produced from fossil carbon source [1-2].

In this concern, the production of dimethyl ether (DME) via CO<sub>2</sub> hydrogenation permits to obtain an alternative and sustainable Diesel fuel [3-5].

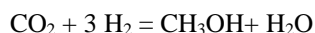
Actually DME is produced from fossil-derived syngas, through two gas-phase routes according to the indirect or direct synthesis path. In the indirect route, methanol (MeOH) is synthesized by CO hydrogenation over conventional Cu/ZnO/Al<sub>2</sub>O<sub>3</sub> catalysts and then dehydrated to DME over an acid catalyst in a separate reactor. In the direct route, DME is synthesized from syngas in "one pot" over a bi-functional catalyst under process conditions close to those of methanol synthesis (240–280 °C, 3–7 MPa) [6-8].

The "one-step" route is more efficient than the "double-step" route, mainly because of thermodynamic advantages related to the equilibrium shift of simultaneous reactions (methanol dehydration to DME promotes the syngas conversion) and for a lower overall process cost. In addition, valorization and reusing of carbon dioxide is an important challenge in order to mitigate the growing global warming due to greenhouse gas emission [9-10]. On this account, more and more attention is receiving the synthesis of DME by total or partial replacement of CO with CO<sub>2</sub> [11-16].

In the one-pot CO<sub>2</sub> hydrogenation process, the DME synthesis net reaction is given by the following reaction:

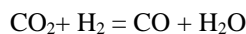


involving the following consecutive steps:



DME synthesis reaction is an exothermic reaction that releases about 122 kJ of heat for each DME mol produced. For this reason, from a thermodynamic point of view, a decrease in reaction temperature should favor the synthesis of DME.

Furthermore, high pressure also should favor DME production since the reaction occurs with a reduction of total moles. Nevertheless, CO<sub>2</sub> is not a highly reactive molecule and temperatures above 240 °C are usually requested for facilitating CO<sub>2</sub> activation rate. High reaction temperature favors endothermic side reactions such as reverse water gas shift:



Furthermore, hydrocarbons and coke may be formed during such process. Therefore, highly active and selective catalyst is required to avoid the formation of undesired by-product. Anyhow, irrespective of the process applied for the DME synthesis, it has been demonstrated that the properties of the acid matrix significantly affect selectivity and durability of bi-functional catalyst as well as the overall process efficiency, being controlled by the dehydration step [17-18].

Several studies have been carried out using  $\gamma$ -Al<sub>2</sub>O<sub>3</sub> as acid catalyst reporting high selectivity towards DME formation in the temperature range 200–300 °C, but also rapid deactivation by water adsorption on Lewis acid sites, especially during the direct synthesis via CO<sub>2</sub> hydrogenation where a lot amount of water is formed from both methanol dehydration and reverse-water-gas-shift reaction [19]. So, a more hydrophobic acid catalyst is suggested to be used in this gas-to-liquid reaction. As alternative to  $\gamma$ -Al<sub>2</sub>O<sub>3</sub>, zeolites have been also investigated revealing a better stability to water and higher methanol conversion [20-24].

Activity, selectivity and stability of zeolites applied in acid-catalyzed reactions are recognized to depend upon several factors as zeolite structure, acidity and crystal size. Zeolite channel system (channel orientation and opening size) is a well-known factor affecting strongly products distribution and catalyst deactivation [25-27].

Acid sites concentration and density, typology (Brønsted and Lewis), strength and location are also important parameters to tune carefully when zeolites are applied in catalysis [28-29].

Furthermore, catalyst resistance to deactivation as well as catalyst effectiveness can be improved by changing size and morphology of zeolite crystals. In particular, application of nano-sized or hierarchical zeolite crystals permits to reduce coke formation and enhance diffusion of reactant species improving catalyst performances [30-31].

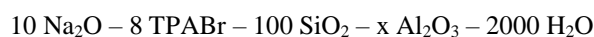
Therefore, the ability of a zeolite to offer chemical-physical properties control in both in situ and post-synthesis treatments is of considerable importance for industrial applications.

FER-type and MFI-type structure disclosed reliable shape-selectivity towards DME synthesis although more details about the role of acid sites should be better elucidate [32-33].

In this paper, a step by step optimization of the catalyst for DME synthesis is reported. The effect of zeolite structure and acidity on methanol dehydration reaction step is assessed by comparing catalytic performances of FER- and MFI-type zeolites with different acidity. Once the best catalyst for methanol dehydration has been identified, the metal/acidic multifunctional catalytic bed configuration was optimized aiming to obtain high DME productivity during one-pot CO<sub>2</sub>-to-DME process.

## 2. MATERIALS AND METHODS

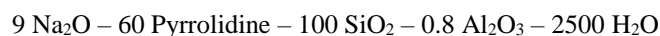
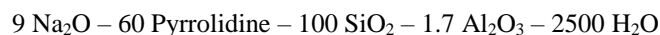
In order to investigate the effect of zeolite features on the DME synthesis, FER-type and MFI-type zeolites with different acidity were synthesized by varying the Si/Al ratio, from 10 to 60. In particular MFI-type zeolites with different acidity level were prepared using tetrapropyl ammonium bromide (TPABr) as structure directing agent (SDA) by starting from a gel with the following molar composition:



where  $x=1, 2$  and  $3.3$  according to the expected Si/Al molar ratio of 15, 25 and 50, respectively.

The crystallization was carried out in a Teflon-lined stainless steel autoclave kept at 175 °C for 5, 4 and 2 days for sample prepared with Si/Al equals to 15, 25 and 50, respectively. Details on the reactants and procedure are reported elsewhere [34].

Pyrrolidine was used as SDA for synthesizing FER-type zeolite with Si/Al=10, whilst pyridine was used for FER30 and FER 60 by adopting the following synthesis molar gel composition, respectively:



Crystallization was carried in a Teflon-lined stainless steel autoclave rotated with a speed of 20 rpm and kept at 175 °C for 3 days for FER (10) and at 165 °C for 5 days for FER (30) and FER (60).

All the crystallized samples were separated from mother liquor by vacuum filtration and washed with distilled water until neutral pH of filtrate was obtained. The solid was dried at 80 °C for 8 h and calcined at 550 °C in air flow with the aim to remove organic molecules. H-form sample was obtained via exchange with NH<sub>4</sub>Cl solution and calcined again at 550 °C in order to eliminate ammonia and to obtain catalyst in acid-form. The obtained H-catalysts were directly used for dimethyl ether synthesis via vapour-phase methanol dehydration. Multifunctional catalysts for one-pot CO<sub>2</sub>-to-DME process were prepared via gel oxalate co-precipitation of CuZnZr nitrate (60/30/10 at.%) in ethanol solutions over H-form zeolite crystals aiming to obtain a hybrid single grain (SG) with CZZ/zeolite with a weight ratio of 1:1. More details about the adopted procedure are reported elsewhere [35]. Furthermore, “homogenous” physical mixtures (PM) constituted by a pre-synthesized CZZ catalyst and a selected zeolite with a weight ratio of 1:1 were also realized.

All of investigated samples were characterized via XRD with APD 2000 Pro diffractometer with a Cu K $\alpha$  radiation (40 kV, 30 mA) in the range 2 theta=5°-50°. The morphology of investigated catalysts was evaluated with both scanning and transmission electron microscopy (SEM – FEI model Inspect, TEM- Philips CM12). Textural properties (e.g. total surface area, micropore volume) were estimated by performing N<sub>2</sub> adsorption/desorption isotherms at 77 K with ASAP 2020 (Micromeritics) instrument. Both NH<sub>3</sub>-TPD and H<sub>2</sub>-TPR analyses were performed according to already published procedures [35].

Vapor-phase methanol dehydration was carried out over H-form zeolites in the temperature range 140-200 °C with a methanol weight hourly space velocity (WHSV) of 4.5 g<sub>MeOH</sub>h<sup>-1</sup> g<sub>cat</sub><sup>-1</sup>, in a lab-scale apparatus described elsewhere [34]. Before each catalytic test, the reactor was purged with nitrogen at 240 °C in order to remove moisture from the catalyst. The catalytic activity of investigated hybrid catalysts during one-pot CO<sub>2</sub>-to-DME hydrogenation reaction was investigated in a fixed-bed reactor at 260 °C and total pressure of 3.0 MPa with a gas hourly space velocity (GHSV) of 8,800 ML/h/g<sub>cat</sub> by feeding a mixture with a CO<sub>2</sub>/H<sub>2</sub>/N<sub>2</sub>=3/9/1 molar ratio. Prior to each test, the catalyst was reduced in situ at 300 °C for 1h under hydrogen flow at atmospheric pressure. For both the processes, reactor stream was analyzed by GC equipped with flame ionized detector (FID) and a thermal conductivity detector (TCD).

### 3. RESULTS AND DISCUSSION

#### 3.1 Characterization

XRD patterns of synthesized zeolites reported in Figure 1 show that both FER-and MFI-type zeolites were obtained with high purity and crystallinity, regardless of aluminum content. After metal co-precipitation no change on both crystallinity and purity was observed.

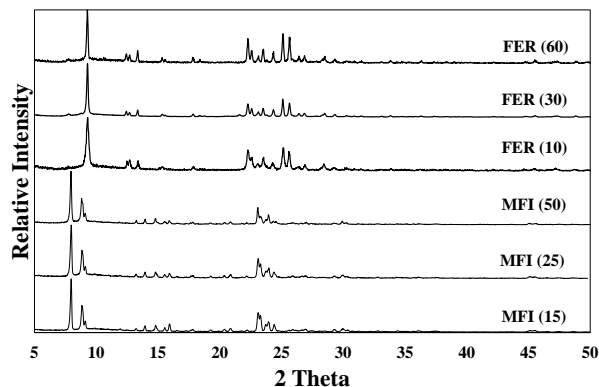


Figure 1. XRD of investigated zeolites

Table 1. Textural properties of investigated materials

Sample	Surface area <sup>1</sup> (m <sup>2</sup> /g)	Micropore volume <sup>2</sup> (cm <sup>3</sup> /g)	d <sub>Cu</sub> <sup>3</sup> (nm)
FER (10)	332	0.126	-
CZZ/FER (10)	217	0.052	4
FER (30)	272	0.108	-
FER (60)	275	0.110	-
MFI (15)	365	0.098	-
MFI (25)	360	0.118	-
MFI (50)	350	0.110	-
CZZ	162	-	11

1. Determined by Brunauer-Emmett-Teller equation

2. Determined by t-plot model

3. Cu average particle size determined by N<sub>2</sub>O chemisorption

Table 2. Acidity properties of investigated materials

Sample	Total acidity <sup>1</sup> (μmol/g)	Weak acid sites <sup>2</sup> (μmol/g)	Strong acid sites <sup>3</sup> (μmol/g)
FER (10)	790	277	513
CZZ/FER (10)	500	140	360
FER (30)	480	67	413
FER (60)	330	36	294
MFI (15)	602	271	331
MFI (25)	515	216	299
MFI (50)	354	159	195

1. Determined from desorbed NH<sub>3</sub> in the temperature range 100-700 °C

2. Determined from desorbed NH<sub>3</sub> in the temperature range 100-300 °C

3. Determined from desorbed NH<sub>3</sub> in the temperature range 300-700 °C

The main textural properties of the investigated materials are reported in Table 1. Both total surface area and micropore volume of bare zeolites are in agreement with the value reported in literature for similar materials. After co-precipitation of metals, both surface area and micropore volume are strongly reduced, probably due to a partial pore blocking of zeolites due to the presence of Cu/Cn/Zr particles. N<sub>2</sub>O

measurements indicate that smaller copper particles are present on FER-type zeolite suggesting that there is some effect of the presence of zeolite on copper dispersion.

Table 2 reports the acidity of investigated samples. Considering bare zeolites, total acidity increases accordingly with aluminium content. Furthermore, MFI-type zeolites disclose a similar fraction of weak (about 45 %) and strong sites (about 55 %). Similar distribution was observed for FER (10). On the contrary, both FER (30) and FER (60) disclose a higher fraction of strong acid sites (more than 85 %). FT-IR analysis (not shown) carried out with both carbon monoxide and D<sub>3</sub>-acetonitrile reveals that only FER (10) possesses Lewis acid sites with a Lewis/Brønsted ratio equals to 0.33, whilst mainly Brønsted acid sites are present on the other FER-and MFI-type samples.

#### 3.2 Catalytic tests

##### (1) Methanol-to-DME

Methanol conversion as a function of reaction temperature for all of investigated zeolites is reported in Figure 2. In the entire range of temperature only DME was observed with no formation of by-products.

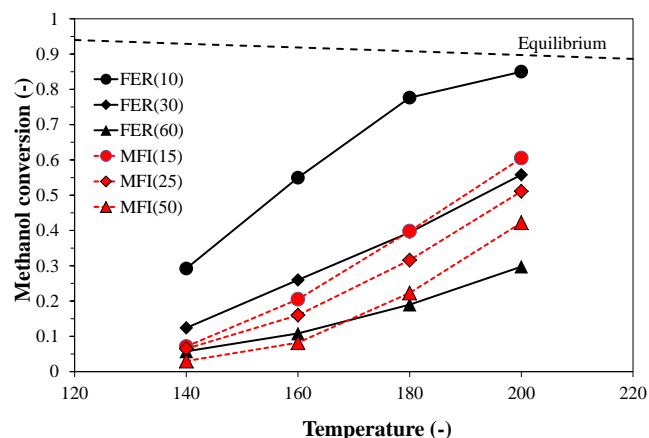


Figure 2. Methanol conversion as a function of reaction temperature for the investigated H-zeolites

Results indicate that catalytic activity during methanol dehydration to DME reaction strongly depends on the acidity of zeolite. In fact, methanol conversion follows the order FER (10)>FER (30)>FER (60) for FER-type zeolites and MFI (15)>MFI (25)>MFI (50) for MFI-type zeolites. On the whole, FER (10) zeolite discloses the highest activity, approaching to the theoretical equilibrium value at the 200 °C, in agreement with the highest value of acidity. On the other hand, although MFI(15) possesses a higher concentration of total acid sites, it shows a lower activity than FER(30) especially at low temperature. Similar behavior is also disclosed for FER (60) and MFI (50) samples. A different trend is observed at temperature higher than 180 °C as both MFI (15) and MFI (50) exhibit a higher activity than FER (30) and FER (60), respectively.

Such behavior may be related to weak/strong acid sites distribution. In fact, the activity order seems to follow strong acid sites concentration at lower temperature and total acid sites concentrations at higher temperature. In fact, it is reasonable to conclude that only strong acid sites are active at lower temperature, whilst weak acid sites became able to catalyze the dehydration of methanol at temperature above or

equals to 180 °C. At this temperature turnover frequency may be then calculated and results are reported in Table 3. Turnover frequency follows the order

FER (10)>FER (30)>MFI (15)>MFI (50)>MFI (25)>FER (60)

revealing that FER (10) and MFI (15) are the most efficient catalysts among the FER-type and MFI-type zeolites, respectively.

Table 3 reports also the apparent activation energies ( $E_{app}$ ) for the investigated catalysts, indicating that the activation barrier is always lower for FER-type materials and it decreases as the total acidity increases.

**Table 3.** Turnover frequency and apparent activation energy of investigated zeolites for methanol-to-DME reaction

Sample	Turnover frequency at 180 °C (mol <sub>DME</sub> /mol <sub>H+</sub> /h)	Apparent activation energy (kJ/mol)
FER (10)	69	38
FER (30)	58	45
FER (60)	41	47
MFI (15)	46	58
MFI (25)	43	62
MFI (50)	44	78

## (2) CO<sub>2</sub>-to-DME

As reported in the previous paragraph, FER (10) may be considered as the most active catalyst for methanol dehydration reaction step, among the investigated FER-type and MFI-type zeolites, respectively. Therefore, one-pot CO<sub>2</sub>-to-DME reaction was carried out at 260 °C and 30 bar by using FER (10) as acid catalyst in three different multifunctional catalytic bed configurations: CZZ-FER (10) dual bed (DB), physical mixture (PM) and hybrid single grain (SG). Figure 3 reports the results of catalytic tests under one-pot CO<sub>2</sub> hydrogenation to DME conditions.

CO<sub>2</sub> conversion is about 18 % for DB system, and it increases at 20 and 22 % for PM and SG systems, respectively. Catalytic tests carried out over CZZ reveal a similar CO<sub>2</sub> conversion and CO selectivity observed for DB system, suggesting that no significant catalytic improvement is obtained when a dual bed is used.

Moreover, reactor bed configuration also strongly affects product distribution.

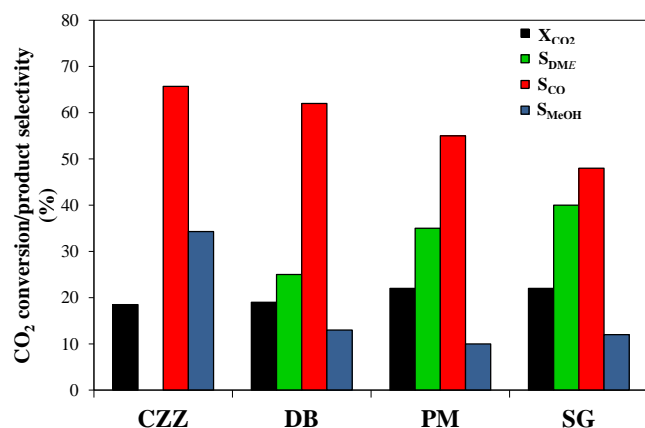


**Figure 3.** CO<sub>2</sub> conversion and selectivity towards DME (S<sub>DME</sub>), CO (S<sub>CO</sub>) and methanol (S<sub>MeOH</sub>) for the investigated CZZ/FER(10)-DB, -PM and -SG systems and CZZ catalyst (T<sub>R</sub>: 260 °C, P<sub>R</sub>: 30 bar, GHSV: 8800 NL/h/g<sub>cat</sub>)

DME selectivity is lower for dual bed reactor that exhibits a DME selectivity of 25 %, meaning that only 5 % of carbon is converted into dimethyl ether. DME selectivity is increased up to 35 % when both CZZ and FER (10) powders are “homogenously” mixed.

When hybrid single grain is used, catalytic performances are further improved, leading to a DME selectivity of 40 %, meaning that more than 10 % of carbon is converted towards the desired product. Such result clearly shows that the efficiency of catalytic bed strongly depends on the possibility to have an intimate cooperation between metallic and acid sites. In that sense, hybrid single grain system should facilitate mass transfer phenomena, so promoting a more rapid dehydration of methanol towards dimethyl ether on neighbouring sites, and bring out the thermodynamic advantages of one-pot process. On the whole, the space-time yield calculated for the investigated system was 732, 640 and 395 g<sub>DME</sub>/h/kg<sub>cat</sub> for SG, PM and DB systems, respectively, again highlighting the crucial role of metal-acid proximity in the synthesis of dimethyl ether.

## 4. CONCLUSIONS

In this work, FER-type and MFI-type zeolites characterized by different structure and acidity were used as catalysts for the vapor-phase dehydration of methanol into dimethyl ether. A Si/Al ratio as low as 10 in the FER-type zeolites allowed to obtain the best performance, showing a DME turnover frequency of 69 mol<sub>DME</sub>/mol<sub>H+</sub>/h. Among MFI-type zeolites, crystals synthesized with a Si/Al=15 disclose the highest catalytic activity. FER (10) zeolite was then used as acid catalyst for one-pot CO<sub>2</sub> hydrogenation to DME coupled with CuZnZr (CZZ) metallic system. Among several catalytic bed configurations assessed (i.e. dual bed, physical mixture and hybrid single grain), the dual bed reactor resulted to be the less effective configuration, whilst hybrid single grain prepared via gel-oxalate co-precipitation of metal precursors over zeolite crystals exhibited significant better catalytic performance, with a DME productivity of 732g<sub>DME</sub>/h/kg<sub>cat</sub>, almost doubled than that obtained with double bed configuration.

## REFERENCES

- [1] Olah GA. (2005). Beyond oil and gas: The methanol economy. *Angew. Chem. Int. Ed* 44(18): 2636-2639. <https://doi.org/10.1002/anie.200462121>
- [2] Perathoner S, Centi G. (2014). CO<sub>2</sub> recycling: A key strategy to introduce green energy in the chemical production chain. *ChemSusChem* 7(5): 1274-1282. <https://doi.org/10.1002/cssc.201300926>
- [3] Arcoumanis C, Bae C, Crookes R, Kinoshita E. (2008). The potential of di-methyl ether (DME) as an alternative fuel for compression-ignition engines: A review. *Fuel* 87(7): 1014-1030. <https://doi.org/10.1016/j.fuel.2007.06.007>
- [4] Park SH, Lee CS. (2014). Applicability of diemthyl ether (DME) in a compression ignition engine as an alternative fuel. *Energ. Conv. Manag* 86: 848-863. <https://doi.org/10.1016/j.enconman.2014.06.051>
- [5] Semelsberg TA, Borup RL, Greene HL. (2006). Dimethyl ether (DME) as an alternative fuel. *J. Power Sourc* 156(2): 497-511.

- <https://doi.org/10.1016/j.jpowsour.2005.05.082>
- [6] Azizi Z, Rezaeimanesh M, Tohidian T, Rahimpour MR. (2014). Dimethyl ether: A review of technologies and production challenges. *Chem. Eng. Process. Proc. Int* 82: 150-172. <https://doi.org/10.1016/j.ccep.2014.06.007>
- [7] Sun J, Yang G, Yoneyama Y, Tsubaki N. (2014). Catalysis chemistry of dimethyl ether synthesis. *ACS Catal* 4(10): 3346-3356. <https://doi.org/10.1021/cs500967j>
- [8] Yoon ES, Han C. (2009). A review of sustainable energy – recent development and future prospects of dimethyl ether (DME) *Comp. Aid. Chem. Eng.* 27: 169-175. [https://doi.org/10.1016/S1570-7946\(09\)70249-4](https://doi.org/10.1016/S1570-7946(09)70249-4).
- [9] Graves C, Ebbesen SD, Mogensen M, Lackner KS. (2011). Sustainable hydrocarbon fuels by recycling CO<sub>2</sub> and H<sub>2</sub>O with renewable or nuclear energy. *Renew. Sus. Energ. Rev* 15(1): 1-23. <https://doi.org/10.1016/j.rser.2010.07.014>.
- [10] Aresta M, Dibenedetto A, Angelini A. (2013). The changing paradigm in CO<sub>2</sub> utilization. *J. CO<sub>2</sub> Util* 3-4: 65-73. <https://doi.org/10.1016/j.jcou.2013.08.001>
- [11] Jia G, Tan Y, Han Y. (2006). A comparative study on the thermodynamics of dimethyl ether synthesis from CO hydrogenation and CO<sub>2</sub> hydrogenation. *Ind. Eng. Chem. Res* 45(3): 1152-1159. <https://doi.org/10.1021/ie050499b>
- [12] An X, Zuo YZ, Zhang Q, Wang D, Wang JF. (2008). Dimethyl ether synthesis from CO<sub>2</sub> hydrogenation on a CuO-ZnO-Al<sub>2</sub>O<sub>3</sub>-ZrO<sub>2</sub>/HZSM-5 bifunctional catalyst. *Ind. Eng. Chem. Res* 47(17): 6547-6554. <https://doi.org/10.1021/ie800777t>
- [13] Bourzutschky JA, Homs N, Bell AT. (1990). Hydrogenation of CO<sub>2</sub> and CO<sub>2</sub>/CO mixtures over copper-containing catalysts. *J. Catal* 124(1): 73-85. [https://doi.org/10.1016/0021-9517\(90\)90104-R](https://doi.org/10.1016/0021-9517(90)90104-R)
- [14] Brown DM, Bhatt BL, Hsiung TH, Lewnard JJ, Waller FJ. (1991). Novel technology for the synthesis of dimethyl ether from syngas. *Catal. Today* 8(3): 279-304. [https://doi.org/10.1016/0920-5861\(91\)80055-E](https://doi.org/10.1016/0920-5861(91)80055-E)
- [15] Olah GA, Goepfert A, Prakash GK. (2009). Chemical recycling of carbon dioxide to methanol and dimethyl ether: from greenhouse gas to renewable, environmentally carbon neutral fuels and synthetic hydrocarbons. *J. Org. Chem* 74(2): 487-498. <https://doi.org/10.1021/jo801260f>
- [16] Li Y, Wang T, Yin X, Wu C, Ma L, Li H, Lv Y, Sun L. (2010). 100 t/a-scale demonstration of direct dimethyl ether synthesis from corn-cob-derived syngas. *Ren. Energ.* 35(3): 583-587. <https://doi.org/10.1016/j.renene.2009.08.002>.
- [17] Ge Q, Huang Y, Qiu F, Li S. (1998). Bifunctional catalysts for conversion of synthesis gas to dimethyl ether. *Appl. Catal. A: Gen* 167(1): 23-30. [https://doi.org/10.1016/S0926-860X\(97\)00290-1](https://doi.org/10.1016/S0926-860X(97)00290-1)
- [18] Catizzzone E, Bonura G, Migliori M, Frusteri F, Giordano G. (2018). CO<sub>2</sub> recycling to dimethyl ether: state-of-the-art and perspectives. *Molecules* 23(1): 31-58. <https://doi.org/10.3390/molecules23010031>
- [19] Sierra I, Erena J, Aguayo T, Olazar M, Bilbao, J. (2010). Deactivation kinetics for direct dimethyl ether synthesis on a CuO-ZnO-Al<sub>2</sub>O<sub>3</sub>/γ-Al<sub>2</sub>O<sub>3</sub> catalysts. *Ind. Eng. Chem. Res* vol. 49(2): 481-489. <https://doi.org/10.1021/ie900978a>
- [20] Naik SP, Ryu T, Bui V, Miller JD, Drinnan N, Zmierczak W. (2011). Synthesis of DME from CO<sub>2</sub>/H<sub>2</sub> gas mixture. *Chem. Eng. J* 167(1): 362-368. <https://doi.org/10.1016/j.ccej.2010.12.087>
- [21] Abu-Dahrieh J, Rooney D, Goguet A, Saih Y. (2012). Activity and deactivation studies for direct dimethyl ether synthesis using CuO-ZnO-Al<sub>2</sub>O<sub>3</sub> with NH<sub>4</sub>ZSM-5, HZSM-5 or γ-Al<sub>2</sub>O<sub>3</sub>. *Chem. Eng. J* 203(1): 201-211. <https://doi.org/10.1016/j.ccej.2012.07.011>
- [22] Bonura G, Migliori M, Frusteri L, Cannilla C, Catizzzone E, Giordano G, Frusteri, F. (2018). Acidity control of zeolite functionality on activity and stability of hybrid catalysts during DME production via CO<sub>2</sub> hydrogenation. *J. CO<sub>2</sub> Util* 24: 398-406. <https://doi.org/10.1016/j.jcou.2018.01.028>
- [23] Bonura G, Frusteri F, Cannilla C, DragoFerrante G, Aloise A, Catizzzone E, Migliori M, Giordano G. (2016). Catalytic features of CuZnZr-zeolite hybrid systems for the direct CO<sub>2</sub>-to-DME hydrogenation reaction. *Catal. Today* 277: 48-54. <https://doi.org/10.1016/j.cattod.2016.02.013>
- [24] Catizzzone E, Migliori M, Purita A, Giordano G. (2019). Ferrierite vs. γ-Al<sub>2</sub>O<sub>3</sub>: The superiority of zeolites in terms of water-resistance in vapour-phase dehydration of methanol to dimethyl ether. *J. Energ. Chem* 30: 162-169. <https://doi.org/10.1016/j.jechem.2018.05.004>
- [25] Migliori M, Catizzzone E, Aloise A, Bonura G, Gomez-Hortiguera L, Frusteri L, Cannilla C, Frusteri F, Giordano G. (2018). New insights about coke deposition in methanol-to-DME reaction over MOR-, MFI- and FER-type zeolites. *J. Ind. Eng. Chem* 68: 196-208. <https://doi.org/10.1016/j.jiec.2018.07.046>
- [26] Guisnet M, Magnoux P. (1989). Coking and deactivation of zeolites: Influence of the pore structure. *Appl. Catal* 54(1): 1-27. [https://doi.org/10.1016/S0166-9834\(00\)82350-7](https://doi.org/10.1016/S0166-9834(00)82350-7).
- [27] Derouane EG. (1985). Factor affecting the deactivation of zeolites by coking. *Stud. Surf. Sci. Catal* 20: 221-240. [https://doi.org/10.1016/S0167-2991\(09\)60173-7](https://doi.org/10.1016/S0167-2991(09)60173-7)
- [28] Corma A. (1995). Inorganic solid acids and their use in acid-catalyzed hydrocarbon reactions. *Chem. Rev* 95: 559-614. <https://doi.org/10.1021/cr00035a006>
- [29] Corma A. (2003). State of the art and future challenges of zeolites as catalysts. *J. Catal* 216(1-2): 298-312. [https://doi.org/10.1016/S0021-9517\(02\)00132-X](https://doi.org/10.1016/S0021-9517(02)00132-X)
- [30] Catizzzone E, Migliori M, Aloise A, Lamberti R, Giordano G. (2019). Hierarchical low Si/Al ratio ferrierite zeolite by sequential postsynthesis treatment: catalytic assessment in dehydration reaction of methanol. *J. Chem* 2019. <https://doi.org/10.1155/2019/3084356>
- [31] Catizzzone E, Van DS, Bianco M, Di-Michele A, Aloise A, Migliori M, Valtchev V, Giordano, G. (2019). Catalytic application of ferrierite nanocrystals in vapour-phase dehydration of methanol to dimethyl ether. *Appl. Catal. B: Env* 243: 273-282. <https://doi.org/10.1016/j.apcatb.2018.10.060>
- [32] Prasad PS, Bae JW, Kang SH, Lee YJ, Jun KW. (2008). Single-step synthesis of DME from syngas on Cu-ZnO-Al<sub>2</sub>O<sub>3</sub>/zeolite bifunctional catalysts: The superiority of ferrierite over the other zeolites. *Fuel Process. Technol* 89(12): 1281-1286. <https://doi.org/10.1016/j.fuproc.2008.07.014>.
- [33] Catizzzone E, Aloise A, Migliori M, Giordano G. (2007). From 1-D to 3-D zeolite structures: performance assessment in catalysis of vapour-phase methanol

- dehydration to DME. *Microp. Mesopo. Mater* 243: 102-111. <https://doi.org/10.1016/j.micromeso.2017.02.022>
- [34] Migliori M, Aloise A, Catizzone E, Giordano G. (2014). Kinetic analysis of methanol to dimethyl ether reaction over H-MFI catalysts. *Ind. Eng. Chem. Res* 53(38): 14885-14891. <https://doi.org/10.1021/ie502775u>
- [35] Bonura G, Cannill C, Frusteri L, Mezzapica A, Frusteri F. (2017). DME production by CO<sub>2</sub> hydrogenation: key factors affecting the behaviour of CuZnZr/ferrierite catalysts. *Catal. Today* 281(1): 337-344. <https://doi.org/10.1016/j.cattod.2016.05.057>